Shape and area fluctuation effects on nucleation theory

Santi Prestipino' , Alessandro Laio' , and Erio Tosatti'

Citation: The Journal of Chemical Physics **140**, 094501 (2014); doi: 10.1063/1.4866971
View online: http://dx.doi.org/10.1063/1.4866971
View Table of Contents: http://aip.scitation.org/toc/jcp/140/9
Published by the American Institute of Physics

Shape and area fluctuation effects on nucleation theory

Santi Prestipino,[1,a)] Alessandro Laio,[2,b)] and Erio Tosatti[2,3,c)]
[1]*Università degli Studi di Messina, Dipartimento di Fisica e di Scienze della Terra, Contrada Papardo, I-98166 Messina, Italy*
[2]*International School for Advanced Studies (SISSA) and UOS Democritos, CNR-IOM, Via Bonomea 265, I-34136 Trieste, Italy*
[3]*The Abdus Salam International Centre for Theoretical Physics (ICTP), P.O. Box 586, I-34151 Trieste, Italy*

(Received 4 November 2013; accepted 14 February 2014; published online 3 March 2014)

In standard nucleation theory, the nucleation process is characterized by computing $\Delta\Omega(V)$, the reversible work required to form a cluster of volume V of the stable phase inside the metastable mother phase. However, other quantities besides the volume could play a role in the free energy of cluster formation, and this will in turn affect the nucleation barrier and the shape of the nucleus. Here we exploit our recently introduced mesoscopic theory of nucleation to compute the free energy cost of a nearly spherical cluster of volume V and a fluctuating surface area A, whereby the maximum of $\Delta\Omega(V)$ is replaced by a saddle point in $\Delta\Omega(V, A)$. Compared to the simpler theory based on volume only, the barrier height of $\Delta\Omega(V, A)$ at the transition state is systematically larger by a few k_BT. More importantly, we show that, depending on the physical situation, the most probable shape of the nucleus may be highly non-spherical, even when the surface tension and stiffness of the model are isotropic. Interestingly, these shape fluctuations do not influence or modify the standard Classical Nucleation Theory manner of extracting the interface tension from the logarithm of the nucleation rate near coexistence. © *2014 AIP Publishing LLC*. [http://dx.doi.org/10.1063/1.4866971]

I. INTRODUCTION

When in a first-order phase transition a thermodynamic phase turns metastable, it may remain stuck for long in a state of apparent equilibrium until a favorable fluctuation triggers the formation of the truly stable phase. Nucleation concerns the early stages of the phase transformation, which initially occurs as an activated process.[1] Despite many attempts to formulate a quantitatively accurate theory of homogeneous nucleation, the important problem of relating the nucleation rate (the main experimentally accessible quantity) to the microscopic features of the system still remains open. A less ambitious program is to find a simple statistical model where a number of nucleation-related issues can find at least a partial answer. In a pair of recent papers,[2,3] we focused on a mesoscopic scale model of this sort, in the form of a field theory in the surface of the nucleating cluster. While the classical nucleation theory (CNT) envisages the cluster surface as sharp and spherical with the same interface free energy as the bulk-coexistence interface, the cluster of our theory can make excursions around a reference shape, with a cost expressed in terms of the parameters of a Landau free energy. Within this theory, two main results were obtained: (i) The cluster formation energy shows, in addition to Landau-type corrections reflecting the finite width of the cluster interface,[4] a term logarithmic in the cluster volume V, with a numerical prefactor whose magnitude *and sign* are only sensitive to the extent of interface anisotropy; (ii) The subleading corrections to the CNT free energy can so much affect the steady-state nucleation rate that the customary way of extracting the interface tension from it, based on the standard CNT recipe may easily lead to wrong results.

Here we pose another question, and give a detailed answer still in terms of our theory, concerning the role of the *area A* of the nucleation cluster. A central assumption in CNT is that a single reaction coordinate (the cluster size or volume) is sufficient to describe the nucleation cluster. This is so frequently and commonly adopted that it is not always appreciated that such a hypothesis is actually only a convenient approximation. To be sure, there exist many notable exceptions. In Refs. 5–11, microscopic attempts were described that go beyond a single reaction coordinate, with important additional insights into the actual mechanism of nucleation. In atomistic simulations in particular, nucleation can be monitored by means of convenient order parameters and the nucleation landscape can be mapped out in terms of these variables. A general finding is the extreme irregularity of cluster shapes which, generally far from spherical, are neither compact nor necessarily one-phase objects. However, atomistic studies are numerical in nature, and therefore intrinsically system-specific.

In this paper, we base on a generic field theory description a study of the modifications in the energetics of nucleation when, besides the cluster volume, the surface area is introduced as a reaction variable. Notwithstanding the simpler and necessarily more abstract nature of our approach compared with atomistic ones, we show that this additional variable, the area, is in many cases irrelevant for the nucleation process, but becomes important when the activation barrier to nucleation is small. The instantaneous and average surface

a)Author to whom correspondence should be addressed. Electronic mail: sprestipino@unime.it
b)E-mail: laio@sissa.it
c)E-mail: tosatti@sissa.it

area of the nucleus are significantly larger than that of the sphere of same volume. Moreover, the free-energy barrier corresponding to the nucleation process is systematically underestimated if one considers only the volume as a reaction variable. We also provide a quantitative estimate of these effects as a function of the model parameters, and inquire whether the standard CNT procedure of extracting the interface free energy from the logarithm of the nucleation rate is going to be affected by an average cluster area larger than spherical.

The paper is organized as follows. In Secs. II and III, we briefly recollect the features and main results of the field theory at the basis of our calculations. Next, in Sec. IV, we present data for the nucleation landscape as a function of volume and area of the cluster. The dependence of the critical size and the barrier height on the model parameters are investigated in detail. In Sec. V, we address the issue how to extract the interface tension from the measured nucleation rate in the light of our new results. Final remarks and conclusions are given in Sec. VI.

II. REVIEW OF THE MODEL

In Refs. 2 and 3, we introduced a model description of the free energy of a homogeneous nucleation cluster as a function of the cluster volume V. The theory goes beyond CNT, in that it allows for fluctuations of the cluster surface Σ around its mean shape. Two cases were considered, both amenable to analytic treatment. A quasispherical cluster, corresponding to an isotropic interface, and a cuboidal cluster, addressing the opposite limit of strongly anisotropic interface tension. We make use of the same theory here, to address the area dependence of the cluster-free energy cost of a nearly spherical cluster.

We first introduce the relevant thermodynamic framework, slightly deviating from the notation used in Refs. 2 and 3. Let the metastable and stable phases be called, respectively, 1 and 2 (for instance, supercooled liquid and solid close to melting). If the basic variable, or reaction coordinate, is chosen to be the volume $\mathcal{V}$ of the phase 2 cluster, then the external control parameters are the temperature T, the volume $V_{\rm tot}$ of the vessel, and the chemical potential μ. Let further P_1 and P_2 be the equilibrium pressure values in the two infinite phases for the given T and μ values. For example, slightly below the coexistence temperature T_m and for $\mu = \mu_m$, the chemical potential value at coexistence, $\Delta P \equiv P_2 - P_1$ is roughly equal to $-L_m/(V_{\rm tot}T_m)\Delta T$, where $\Delta T = T - T_m$ and L_m is the heat of fusion. In a long-lived metastable 1 state not far from coexistence, shape fluctuations of the 1-2 interface in a cluster of phase 2 occur with a weight proportional to the Boltzmann factor relative to a coarse-grained Hamiltonian $\mathcal{H}[\Sigma]$ (here, a Landau grand potential), given by

$$\mathcal{H}[\Sigma] = -P_1(V_{\rm tot} - \mathcal{V}[\Sigma]) - P_2\mathcal{V}[\Sigma] + \mathcal{H}_s[\Sigma], \qquad (2.1)$$

where $\mathcal{V}[\Sigma]$ is the cluster volume enclosed by Σ and $\mathcal{H}_s[\Sigma]$ is the free-energy functional accounting for the cost of the interface (note that, at this level of generality, it is not even necessary that Σ be a connected surface).

For the $\mathcal{H}_s[\Sigma]$ in Eq. (2.1), we assume a Canham-Helfrich form, containing spontaneous-curvature and bending-energy terms in addition to interface tension, with parameters derived from a more fundamental Landau free energy. In detail, denoting by H the mean curvature of the surface Σ of the cluster, the interface free-energy functional reads

$$\mathcal{H}_s[\Sigma] = \int_\Sigma {\rm d}S\, \left(\sigma_m - 2\sigma_m\delta_m H + 2\lambda H^2\right), \qquad (2.2)$$

where the system-specific quantities σ_m, δ_m, and λ would generally depend on the local surface orientation (see the form of these coefficients in Ref. 3).

As mentioned above, two limiting cases of Eq. (2.2) can be studied analytically, those of isotropic and of extremely anisotropic interfaces. In the isotropic case, σ_m, δ_m, and λ are constant parameters and the shape of the cluster is on average spherical. Although the solid-liquid interface is notoriously anisotropic, in many cases (hard spheres, Lennard-Jones fluid, etc.) the anisotropy is small enough to be neglected as a first step. When deviations from sphericity are small, the equation for Σ can be expressed in spherical coordinates as $R(\theta, \phi) = R_0[1 + \epsilon(\theta, \phi)]$ with $\epsilon(\theta, \phi) \ll 1$. Denoting by $x_{l,m}$, the Fourier coefficients of $\epsilon(\theta, \phi)$ on the basis of real spherical harmonics, and discarding terms of order higher than the second in these coefficients, the functional $\mathcal{H}_s$ takes the explicit form:[3]

$$\begin{aligned}\mathcal{H}_s = {} & 4\pi\sigma_m R_0^2 + \frac{\sigma_m R_0^2}{2}\sum_{l>0,m}(l^2 + l + 2)x_{l,m}^2 - 8\pi\sigma_m\delta_m R_0 \\ & - \sigma_m\delta_m R_0 \sum_{l>0,m} l(l+1)x_{l,m}^2 + 8\pi\lambda \\ & + \frac{\lambda}{2}\sum_{l>1,m} l(l+1)(l-1)(l+2)x_{l,m}^2. \end{aligned} \qquad (2.3)$$

III. NUCLEATION CLUSTER OF VOLUME V AND AREA A: THE RESTRICTED GRAND POTENTIAL

The model described by Eqs. (2.1) and (2.2) assumes that the relevant collective variable (CV) for describing the process is the volume V of the nascent cluster. Under this assumption, the relevant thermodynamic potential is the restricted grand potential for a predominantly 1 system with an inclusion of phase 2 of arbitrary shape but fixed volume V:

$$\Omega_{1+2}(V) = -\frac{1}{\beta}\ln\left\{a^3\int \mathcal{D}\Sigma\, \delta(\mathcal{V}[\Sigma] - V)e^{-\beta\mathcal{H}[\Sigma]}\right\}, \qquad (3.1)$$

where, on the right-hand side, $\beta = (k_B T)^{-1}$. In Eq. (3.1), a is a microscopic length and $\mathcal{D}\Sigma$ is a dimensionless integral measure. For the same choice of eigenfunctions as in Eq. (2.3), the integral measure reads[3]

$$\int \mathcal{D}\Sigma = \int_{-\infty}^{+\infty}\prod_{l>0,m}\left(\frac{S}{s}\,{\rm d}x_{l,m}\right)\int_0^{+\infty}\frac{{\rm d}R_0}{a}, \qquad (3.2)$$

where $S = (36\pi)^{1/3}V^{2/3}$ is the area of the spherical surface of volume V and $s = 4\pi a^2$. We emphasize that, due to the existence of a lower cutoff of a on interparticle distances, a l upper

cutoff of $l_{\max} = \sqrt{S}/a - 1$ is implicit in Eq. (3.2). Hence, V cannot take any values but only those related to $l_{\max}$ via

$$(36\pi)^{1/3} V^{2/3} = S = (l_{\max} + 1)^2 a^2, \quad l_{\max} = 2, 3, 4, \ldots. \tag{3.3}$$

The grand potential of 1 is simply $\Omega_1 = -P_1 V_{\rm tot}$, although a different but equivalent expression is also possible, considering that, by its very nature, phase 1 contains small clusters of phase 2 in its interior. Denoting $V_{\max}$ the maximum volume an inclusion of 2 can have without altering the nature of 1, we can also write

$$\Omega_1 = -\frac{1}{\beta} \ln \int_{\mathcal{V}[\Sigma] < V_{\max}} \mathcal{D}\Sigma \, e^{-\beta \mathcal{H}[\Sigma]} \tag{3.4}$$

(the value of $V_{\max}$ is close above the critical volume V^*, i.e., the volume in the transition state).

The grand-potential excess $\Delta\Omega(V)$, providing the reversible/minimum work needed to form a 2-phase inclusion of volume V within 1, is evaluated as

$$\begin{aligned} \Delta\Omega(V) &\equiv \Omega_{1+2}(V) - \Omega_1 = (P_1 - P_2)V \\ &\quad - \frac{1}{\beta} \ln \left\{ a^3 \int \mathcal{D}\Sigma \, \delta(\mathcal{V}[\Sigma] - V) e^{-\beta \mathcal{H}_s[\Sigma]} \right\} \\ &\equiv -V \Delta P + F_s(V), \end{aligned} \tag{3.5}$$

$F_s(V)$ being the surface free energy. Equation (3.5) resembles the free-energy barrier of CNT, with the key difference that the CNT cost for the surface is only the leading term in $F_s(V)$. Finally, there is a simple relation between $\Delta\Omega(V)$ and the probability density of volume, defined as

$$\rho(V) \equiv \frac{\int \mathcal{D}\Sigma \, \delta(\mathcal{V}[\Sigma] - V) \exp\{-\beta \mathcal{H}[\Sigma]\}}{\int_{\mathcal{V}[\Sigma] < V_{\max}} \mathcal{D}\Sigma \, \exp\{-\beta \mathcal{H}[\Sigma]\}}. \tag{3.6}$$

Using Eqs. (3.1) and (3.4), it promptly follows that

$$-\frac{1}{\beta} \ln \left\{ \rho(V) a^3 \right\} = \Delta\Omega(V), \tag{3.7}$$

which provides a way to calculate $\Delta\Omega$ numerically.[12–14] Simulations show that, unless V is very small, an overwhelming fraction of 2 particles is gathered in a single cluster, as indeed expected from the arguments in Ref. 15. A connected 2-phase inclusion within 1 is also a leading assumption of the theory of Refs. 2 and 3.

With these stipulations, the free-energy cost of cluster formation for large V turns out to be

$$\Delta\Omega(V) = -V \Delta P + \widetilde{A} \, V^{2/3} + \widetilde{B} \, V^{1/3} + \widetilde{C} - \frac{7}{9} k_B T \ln \frac{V}{a^3}, \tag{3.8}$$

with $\widetilde{A}, \widetilde{B}, \widetilde{C}$ explicit functions of σ_m, δ_m, and λ given in Ref 3. Equation (3.8) represents a step forward from CNT, as confirmed by explicit simulations in the Ising model.[2,3]

Here we proceed to characterize the quasispherical cluster by means of a coarse-grained free energy function where, besides the volume, we use the area A of the cluster surface as a second CV:

$$\begin{aligned} &\Delta\Omega(V, A) \\ &= -k_B T \ln \left\{ a^5 \int \mathcal{D}\Sigma \, \delta(\mathcal{V}[\Sigma] - V) \delta(\mathcal{A}[\Sigma] - A) e^{-\beta \mathcal{H}[\Sigma]} \right\} \\ &\equiv -V \Delta P + F_s(V, A). \end{aligned} \tag{3.9}$$

The meaning of $\Delta\Omega(V, A)$ is the cost of forming a solid cluster of area A and volume V out of the liquid. The last term in (3.9) (i.e., the surface free energy) is given by

$$e^{-\beta F_s(V,A)} = a^5 \int \mathcal{D}\Sigma \, \delta(\mathcal{V}[\Sigma] - V) \delta(\mathcal{A}[\Sigma] - A) e^{-\beta \mathcal{H}_s}, \tag{3.10}$$

and the following sum rule holds:

$$\int_0^{+\infty} \frac{\mathrm{d}A}{a^2} \, e^{-\beta \Delta\Omega(V,A)} = e^{-\beta \Delta\Omega(V)}, \tag{3.11}$$

which provides a useful consistency check of the calculation.

We proceed as for the earlier computation of $\Delta\Omega(V)$ in Ref. 3, by first carrying out the trivial integral over R_0. The result is

$$\begin{aligned} &e^{-\beta F_s(V,A)} \\ &= (36\pi)^{-2/3} \left(\frac{V}{a^3} \right)^{-4/3} e^{-8\pi\beta\lambda} e^{8\pi\beta\sigma_m\delta_m (3V/(4\pi))^{1/3}} e^{-\beta\sigma_m A} \\ &\quad \times \int_{-\infty}^{+\infty} \prod_{l>0,m} \left(\frac{S}{s} \mathrm{d}x_{l,m} \right) \exp\left(-\frac{1}{4\pi} \sum_{l>0,m} x_{l,m}^2 \right) \\ &\quad \times \exp\left(-\frac{\beta\lambda}{2} \sum_{l>1,m} l(l+1)(l-1)(l+2) x_{l,m}^2 \right) \\ &\quad \times \exp\left(\beta\sigma_m\delta_m \left(\frac{S}{4\pi} \right)^{1/2} \sum_{l>1,m} (l^2 + l - 2) x_{l,m}^2 \right) \\ &\quad \times \delta\left(1 + \frac{1}{8\pi} \sum_{l>1,m} (l^2 + l - 2) x_{l,m}^2 - (36\pi)^{-1/3} V^{-2/3} A \right). \end{aligned} \tag{3.12}$$

Note that the delta-function argument is strictly positive for $A < (36\pi)^{1/3} V^{2/3}$, yielding in this case $F_s(V, A) = +\infty$. This just expresses the well-known fact that the sphere has the smallest surface area among all surfaces enclosing a given volume. Hence, we take $A > (36\pi)^{1/3} V^{2/3}$ in the following and define the deviation from sphericity as

$$\alpha \equiv (36\pi)^{-1/3} V^{-2/3} A - 1 > 0. \tag{3.13}$$

Using the integral representation of the delta function, we obtain

$$
\begin{aligned}
e^{-\beta F_s(V,A)} &= (36\pi)^{-2/3}\left(\frac{V}{a^3}\right)^{-4/3} e^{-8\pi\beta\lambda} e^{8\pi\beta\sigma_m\delta_m(3V/(4\pi))^{1/3}} e^{-\beta\sigma_m A}\,\frac{1}{2\pi}\int_{-\infty}^{+\infty} \mathrm{d}k\, e^{-i\alpha k} \\
&\times \int_{-\infty}^{+\infty} \prod_{l>0,m}\left(\frac{S}{s}\mathrm{d}x_{l,m}\right) \exp\left\{-\frac{1}{4\pi}\sum_{l>0,m}\left[1+2\pi\beta\lambda\, l(l+1)(l-1)(l+2)\right.\right. \\
&\left.\left. -4\pi\beta\sigma_m\delta_m\left(\frac{S}{4\pi}\right)^{1/2}(l^2+l-2)-\frac{i}{2}(l^2+l-2)k\right]x_{l,m}^2\right\} \\
&= (36\pi)^{-2/3}\left(\frac{V}{a^3}\right)^{-4/3} e^{-8\pi\beta\lambda} e^{8\pi\beta\sigma_m\delta_m(3V/(4\pi))^{1/3}} e^{-\beta\sigma_m A}\left(\frac{2\pi S}{s}\right)^{\sum_{l=1}^{l_{\max}}(2l+1)} \\
&\times \frac{1}{2\pi}\int_{-\infty}^{+\infty}\mathrm{d}x\,\frac{e^{-i\alpha x}}{\prod_{l=2}^{l_{\max}}\left\{c_l(S)-\frac{i}{2}(l^2+l-2)x\right\}^{(2l+1)/2}},
\end{aligned}
\tag{3.14}
$$

where

$$
\begin{aligned}
c_l(S) &= 1+2\pi\beta\lambda\, l(l+1)(l-1)(l+2) \\
&\quad -4\pi\beta\sigma_m\delta_m(l^2+l-2)\left(\frac{S}{4\pi}\right)^{1/2}.
\end{aligned}
\tag{3.15}
$$

The last step in (3.14) is only justified when all $c_l(S) > 0$. A problem then occurs for $\delta_m > 0$ since, above a certain value of the volume, $c_2(S)$ becomes negative and $F_s(V, A)$ ceases to be defined. For $l_{\max} = 2$, the integral in (3.14) can be evaluated analytically (see Appendix A). In the other cases, this integral is best converted into a real integral,

$$
\begin{aligned}
&\int_{-\infty}^{+\infty}\mathrm{d}x\,\frac{e^{-i\alpha x}}{\prod_{l=2}^{l_{\max}}\left\{c_l(S)-\frac{i}{2}(l^2+l-2)x\right\}^{(2l+1)/2}} \\
&= 2\prod_{l=2}^{l_{\max}} c_l(S)^{-(2l+1)/2} \\
&\times \int_0^{+\infty}\mathrm{d}x\,\frac{\cos\left[\alpha x-\sum_{l=2}^{l_{\max}}\frac{2l+1}{2}\arctan\left(\frac{l^2+l-2}{2}\frac{x}{c_l(S)}\right)\right]}{\prod_{l=2}^{l_{\max}}\left[1+\left(\frac{l^2+l-2}{2}\frac{x}{c_l(S)}\right)^2\right]^{(2l+1)/4}},
\end{aligned}
\tag{3.16}
$$

which is easier to compute numerically. We used Eq. (3.16) to evaluate $\Delta\Omega(V, A)$ up to $l_{\max} = 14$ for a number of combinations of the model parameters.

IV. RESULTS

In Fig. 1, we plot the contour lines of $\Delta\Omega(V, A)$ in the (V, α) plane for a specific yet arbitrary choice of model parameters. A clear saddle point is seen on the free-energy surface, marked by an asterisk in the lower panel of Fig. 1. The transition state for nucleation is nothing but this free-energy saddle, which is the "mountain pass" separating the basin of attraction of the liquid ($V = 0$) from the region of (V, A) points which, under the system dynamics, would flow downhill to the "solid" sink at $V = +\infty$.

When averaged over many different dynamical trajectories, the nucleation process can be described as following the lowest-free-energy route since the Boltzmann weight is highest at the bottom of the free-energy valley. However, due to the statistical nature of nucleation, individual nucleation events also involve some excursions up the walls of the valley, which are more frequent on the high-α side because of the far more numerous shapes available there for the cluster. In

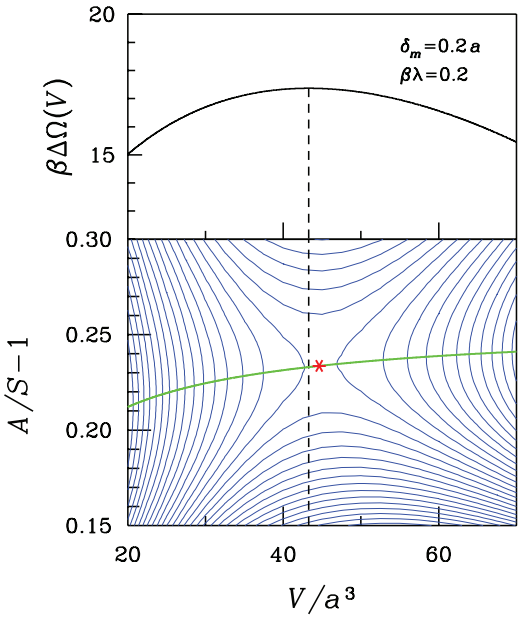

FIG. 1. Quasispherical cluster: $\Delta\Omega(V)$ (top) and $\Delta\Omega(V, A)$ (bottom) in units of k_BT, for a specific set of model parameters ($\beta\Delta P a^3 = 1$, $\beta\sigma_m a^2 = 1$, $\delta_m = 0.2\,a$, and $\beta\lambda = 0.2$). For these as well as other values of the parameters, we have checked by visual inspection that $\Delta\Omega(V, A)$ is indeed a concave function of V and a convex function of A (and of α as well). To have a better view of the figure, the two-dimensional nucleation landscape has been represented through the contour lines of $\Delta\Omega(V, A)$ in the (V, α) plane. The green solid line in the bottom panel marks the minimum-free-energy path $\alpha_{\min}(V)$. The red asterisk marks the position of the saddle point of $\Delta\Omega(V, A)$ as computed through the interpolation procedure outlined in the text. In the case considered, the critical volume increases by roughly 3% when the second collective variable A is introduced, whereas the barrier height changes from 17.368 to 19.343 (+11%). We checked numerically for $l_{\max} = 3, 4, 5$ that Eq. (3.11) is exactly fulfilled (for $l_{\max} = 2$ this is done analytically in Appendix A).

particular, uphill excursions on the free-energy surface away from the saddle point along the A direction provide the cost of fluctuations of the nucleus about its mean shape. Clearly, both the most favorable nucleation pathway as well as the extent of corrugations of the nucleus surface above its mean shape vary with the theory parameters. For the case reported in Fig. 1 (and in many other cases as well), the value of α along the minimum-free-energy path increases very slowly with V, apparently approaching a finite value at infinity.

A non-zero saddle-point value of α implies that the nucleus—which is spherical only on average—has ripples in its surface. This is not particularly surprising, considering that it is convenient for the cluster to deviate from perfect sphericity in order to gain entropy from shape fluctuations—a finite-size roughening. The perfect sphere exerts an entropic repulsion on the cluster shape, which is similar to the mechanism at the origin of the free wandering of an interface away from an attractive hard wall above the depinning temperature.[16]

In order to calculate the saddle-point coordinates (V^*, α^*) for given values of the parameters, we first computed the minimum of $\Delta\Omega$ as a function of α for each $l_{\max}$; then, after extending $l_{\max}$ to a continuous variable, we maximized $\Delta\Omega$ along the lowest-free-energy route just determined and eventually converted the result in V units. In a few cases, including the example in Fig. 1, we checked that this procedure gives exactly the same saddle point as revealed by the contour plot.

The main message from Fig. 1 is that the critical volume V^* is larger when allowing for two CVs, (V, A), than for V only. The same holds for $\Delta\Omega^*$. The latter result is true in general as is seen in Fig. 2, which reports one- and two-CV values of V^* and $\Delta\Omega^*$ in a wide range of δ_m, λ, and ΔP. The underlying reason is that the nonlinear procedure of obtaining $\Delta\Omega(V)$ from $\Delta\Omega(V, A)$ by integrating out the A variable (Eq. (3.11)) unavoidably corrupts the critical volume and the barrier height causing both to appear artificially smaller than their true value, unless the minimum free-energy path were exceptionally parallel to the V axis. The impact on V^* and $\Delta\Omega^*$ of treating area as a collective variable besides volume is stronger when the barrier is low, leading to barrier-height increases as large as 15% in the cases plotted (but twice as that for, e.g., $\delta_m = 0.1\,a$, $\beta\lambda = 0.1$, and $\beta\Delta Pa^3 = 1.5$). On the other hand, in most cases the relative changes of V^* and $\Delta\Omega^*$ are only a few percent. This could explain why, in simulations of the Ising model,[5] cluster area was found to play only a minor role in the dynamics of nucleation. As a side note, we observe that the ΔP value at which $\Delta\Omega^*$ would extrapolate to zero is larger in the two-CV case. This suggests that the spinodal threshold is always underestimated in a treatment where only one reaction variable (V) is considered.

Looking at Fig. 2, we see that the behavior of V^* and $\Delta\Omega^*$ is similar. They both increase with reducing δ_m and with increasing λ, as may be expected from the form (2.2) of the interface free-energy functional, which shows that in general a larger cost should be paid for the interface when $-\delta_m$ and λ are larger.

As coexistence is approached, the nucleus becomes effectively flatter, since the mean radial amplitude of the surface ripples, growing as $\sqrt{\ln(V^*/a^3)}$ as expected for a thermodynamically rough interface, becomes negligible in comparison

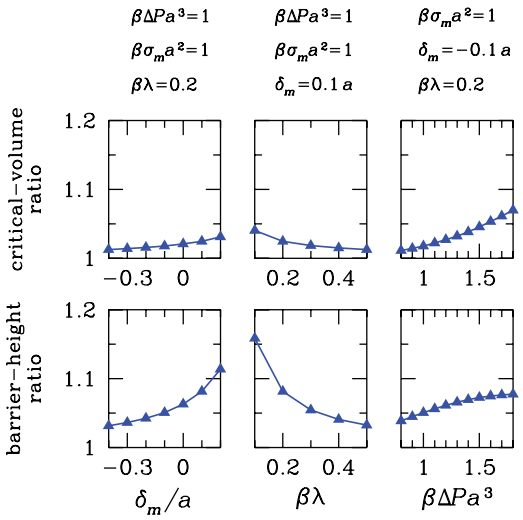

FIG. 2. Top: Ratio between values of the critical volume V^* obtained with (V, A) as collective variables and those obtained with V only, plotted as a function of the three model parameters δ_m, λ, and ΔP—one at a time. Bottom: Same ratio, now between values of the barrier height $\Delta\Omega^*$. The critical volume and the barrier height are both systematically larger in the (V, A) case. Observe that, for $\beta\lambda = 0.2$ and $\delta_m = 0.3\,a$ $(0.4\,a)$, the maximum value of $l_{\max}$ for which the integral in (3.14) still converges is 6 (respectively, 4), i.e., too low to identify a saddle point on $\Delta\Omega(V, A)$.

with the nucleus radius. Despite that, it is not *a priori* clear what the critical area ratio α^* should do in the coexistence limit, where the critical nucleus volume diverges. Upon plotting α^* as a function of supersaturation for fixed values of the other parameters, we see that α^* increases slowly as ΔP is reduced (see Fig. 3), apparently saturating to approach a finite value at coexistence. Hence, we conclude that the weak—even if unlimited—growth of the interface width with volume yields a quantitatively modest residual corrugation of the nucleation cluster which is unable to change the scaling of cluster area from $V^{2/3}$ to a higher power, and apparently even to a

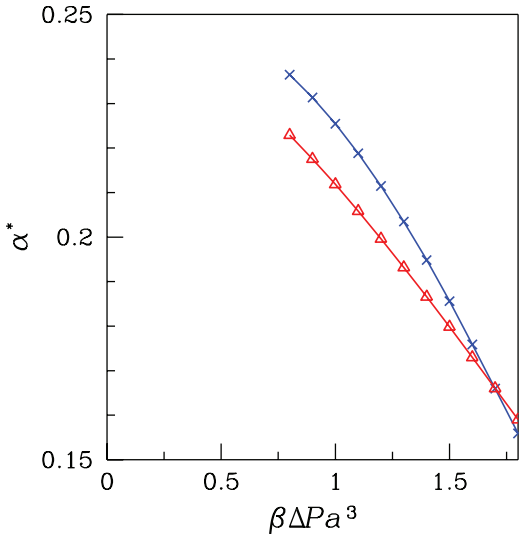

FIG. 3. Quasispherical cluster: Saddle-point value of α, plotted as a function of supersaturation, for $\beta\sigma_m a^2 = 1$ and $\beta\lambda = 0.2$ (blue crosses: $\delta_m = 0.1\,a$; red triangles: $\delta_m = -0.1\,a$). Approaching coexistence, where surface roughening ripples diverge, the ratio of the area of critical clusters to that of the equivalent sphere remains finite ($\approx$1.25).

marginally faster increase such as $V^{2/3}\ln(V/a^3)$. This expectation finds a confirmation in Appendix B, where the mean area of a quasispherical cluster of fixed volume is shown to scale exactly as $V^{2/3}$. Since α^* is roughly equal to the value of $\langle\mathcal{A}\rangle_V/S-1$ for $V=V^*$, we expect the same asymptotic behavior for both quantities.

V. EXTRACTING THE INTERFACE TENSION FROM THE NUCLEATION RATE

Finally, we consider whether employing one (V) or two CVs (V and A) could affect the time-honored CNT extraction procedure of the interface tension at coexistence, σ_∞, from the rate of nucleation I. Assuming the standard transition-state-theory (Arrhenius-like) expression of I for all supersaturations, i.e., $I=I_0\exp\{-\beta\Delta\Omega^*\}$, the most important source of I dependence on ΔP is the exponent, $-\beta\Delta\Omega^*$. The latter quantity is plotted in Fig. 4 for both one- and two-CV cases, and for two different choices of parameters. We point out that the near-coexistence slope of $-\beta\Delta\Omega^*$ is expected to be the same for both one- and two-dimensional surface free energy, see our argument in Appendix C.

According to CNT, $\ln(I/I_0)$ should be a linear function of $(\Delta P)^{-2}$, with a slope proportional to σ_∞^3. In the fluctuating-shape cluster model instead, $\ln(I/I_0)$ is a concave function of $(\Delta P)^{-2}$ ($\delta_m>0$) or a convex one ($\delta_m<0$), with the latter case apparently applying for colloids (see, e.g., Fig. 7(b) of Ref. 17). Hence, as was underlined in Ref. 2, the correct procedure of extracting the interface tension at coexistence entails by necessity an extrapolation of the slope of $\ln(I/I_0)$ at vanishing undercooling, independently of whether we consider only V or (V, A) as CVs.

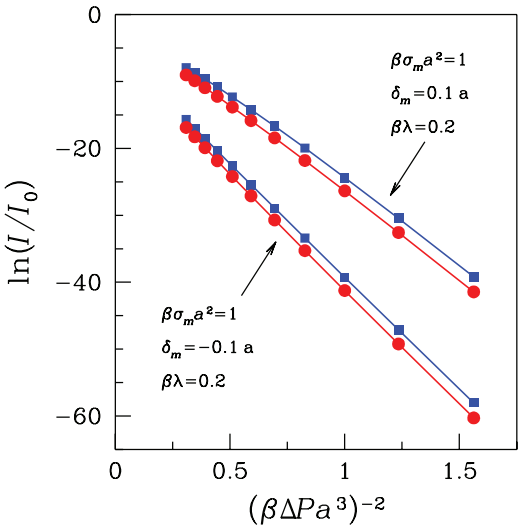

FIG. 4. Quasispherical cluster for $\beta\sigma_m a^2=1$ and $\beta\lambda=0.2$, and for two opposite values of δ_m. We plot $-\beta\Delta\Omega^*$ as a function of $(\Delta P)^{-2}$, which represents the leading ΔP dependence of $\ln I$ (blue squares: one-CV case; red dots: two-CV case). The slope of $\ln(I/I_0)$ is nearly constant (i.e., CNT-like) only for very low supersaturations. In this limit the slope of $\ln(I/I_0)$ appears to be the same for both one- and two-CV cases (see text and Appendix C, where a proof of this equivalence is provided). We observe that the direction of bending of $\ln I$ as a function of $(\Delta P)^{-2}$ is a reliable marker of the sign of the Tolman length.

Quantitatively, the rate of nucleation is sensitive to the number of CVs employed in the calculation: with two variables instead of one, I is reduced by a few orders of magnitude for low supersaturations.

Since the limiting slope of $\ln I$ is the same for both one and two CVs, a one-CV description of nucleation is sufficient when the only objective is to get σ_∞ out of a model of the nucleation cluster. It is useful here to restate that the "thermodynamical" (i.e., dressed by thermal fluctuations) surface tension σ_∞, rather than the "mechanical" surface tension τ (see Appendix B), is what one obtains from a measurement of the nucleation rate.

VI. CONCLUSIONS

In nucleation, the minimum free-energy cost $\Delta\Omega$ for making a cluster of the stable phase (e.g., solid) out of the metastable parent phase (e.g., liquid) is the sum of two terms: a negative volume term, representing the benefit for switching a region from liquid to solid, and a positive surface term, F_s, which is the cost for creating the interface. A crucial assumption of standard nucleation theories is that the surface free energy F_s only depends on V, the cluster volume; at the critical size, the reversible work of cluster formation reaches a maximum value, which in turn determines the steady-state nucleation rate for low enough undercooling.

Refining the standard description of the free energy of nucleation, we have extended the theory of Refs. 2 and 3 using the area A of the cluster surface as a second collective variable besides volume V. The transition state is now a saddle point in the two-dimensional free-energy surface, and the shape of the nucleus is that of a corrugated sphere whose area relative to the equivalent sphere depends upon the model parameters. We found that the inclusion of area systematically corrects the barrier height upwards by a few k_BT, which in relative terms may be important especially for low barriers. Otherwise, the extrapolation procedure towards coexistence required to extract the interface tension from the nucleation rate remains exactly the same as for the volume-only case. In closing, we also speculate that the effective rugosity, here signaled by the parameter α, might be expected to play a role in modifying the effective Stokes frictional force felt, e.g., by a solid nucleation cluster drifting in a fluid flow.

ACKNOWLEDGMENTS

This project was co-sponsored by the Italian Ministry of Education and Research through Contract No. PRIN/COFIN 2010LLKJBX_004, and by ERC Advanced Grant No. 320796 MODPHYSFRICT. It also benefitted from the research environment and stimulus provided by SNF Sinergia Contract No. CRSII2 136287.

APPENDIX A: CALCULATION OF $\Delta\Omega(V_2, A)$

We here consider in more detail the calculation of $\Delta\Omega(V, A)$ for the case $l_{\max}=2$ (corresponding to $S/a^2=9$ and $V/a^3=9/(2\sqrt{\pi})=2.53885\ldots$), which is perhaps the only case allowing for an analytic treatment. Assuming

$c_2 > 0$, we should compute the following integral:

$$\int_{-\infty}^{+\infty} \mathrm{d}x \, \frac{e^{-i\alpha x}}{(c_2 - 2ix)^{5/2}} = c_2^{-3/2} \int_{-\infty}^{+\infty} \mathrm{d}x \, \frac{e^{-ic_2\alpha\, x}}{(1 - 2ix)^{5/2}} \equiv c_2^{-3/2} I(c_2\alpha), \tag{A1}$$

where

$$I(\alpha) = \int_{-\infty}^{+\infty} \mathrm{d}x \, \frac{e^{-i\alpha x}}{(1 - 2ix)^{5/2}}. \tag{A2}$$

The integrand is a complex function of real variable which does not show singularities on the integration path. Integrating twice by parts, we obtain

$$I = \frac{\alpha^2}{3} \int_{-\infty}^{+\infty} \mathrm{d}x \, \frac{e^{-i\alpha x}}{(1 - 2ix)^{1/2}}. \tag{A3}$$

In order to determine (A3), we consider the complex integral

$$\oint_{\Gamma} \mathrm{d}z \, \frac{e^{-i\alpha z}}{(1 - 2iz)^{1/2}} \tag{A4}$$

over a keyhole circuit Γ of the complex plane, see Fig. 5. The circuit is so chosen as to avoid the singularity of the integrand at $z_0 = -i/2$. Since there are no poles inside Γ, the integral (A4) simply vanishes. On the other hand, the same integral is the sum of various contributions, one of which approaches I in the $L \to +\infty$ limit.

Let Γ_L denote the semicircumference with center in the origin and radius L, lying in the half-plane $\mathrm{Im} z < 0$, and Γ_ϵ the circumference of radius ϵ, centered in z_0. We shall prove later that the integrals over Γ_L and Γ_ϵ both vanish, respectively, in the $L \to +\infty$ and $\epsilon \to 0^+$ limits. As far as the integrals over the segments AB and CD of Fig. 5 are concerned, they are given by

$$\int_{z_0-\delta}^{-iL-\delta} \mathrm{d}z \, \frac{e^{-i\alpha z}}{(1 - 2iz)^{1/2}} \quad \text{and} \quad \int_{-iL+\delta}^{z_0+\delta} \mathrm{d}z \, \frac{e^{-i\alpha z}}{(1 - 2iz)^{1/2}}, \tag{A5}$$

δ being a small positive number.

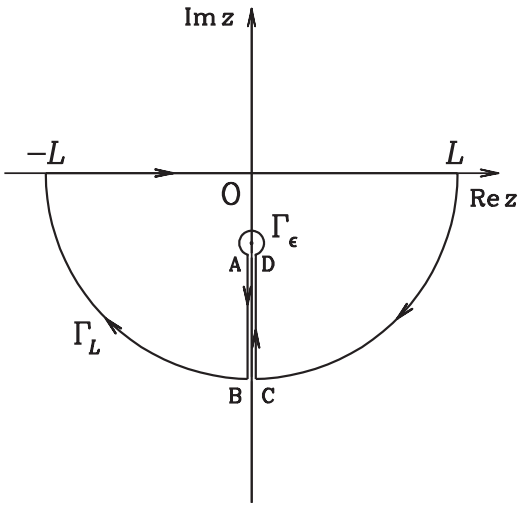

FIG. 5. The integration path Γ that was considered in the evaluation of the integral (A4).

Putting the branch cut of $z^{1/2}$ on the semiaxis of negative reals,

$$z^{1/2} = \exp\left\{\frac{1}{2} \ln_{[-\pi,\pi)} z\right\} = \exp\left\{\frac{1}{2} \left(\ln|z| + i \arg_{[-\pi,\pi)} z\right)\right\}, \tag{A6}$$

and taken $z = -i/2 - it - \delta$, the first integral (A5) becomes

$$-ie^{-\alpha/2} \int_0^{L-1/2} \mathrm{d}t \, \frac{e^{-\alpha t} e^{i\alpha\delta}}{(-2t + 2i\delta)^{1/2}}, \tag{A7}$$

where

$$(-2t + 2i\delta)^{1/2} = \exp\left\{\frac{1}{2}(\ln|-2t + 2i\delta| + \pi i)\right\} \xrightarrow{\delta\to 0^+} i(2t)^{1/2}. \tag{A8}$$

Hence

$$\int_{z_0-\delta}^{-iL-\delta} \mathrm{d}z \, \frac{e^{-i\alpha z}}{(1 - 2iz)^{1/2}} \xrightarrow{\delta\to 0^+} -e^{-\alpha/2} \int_0^{L-1/2} \mathrm{d}t \, \frac{e^{-\alpha t}}{(2t)^{1/2}}. \tag{A9}$$

Similarly, since

$$(-2t - 2i\delta)^{1/2} = \exp\left\{\frac{1}{2}(\ln|-2t-2i\delta| - \pi i)\right\} \xrightarrow{\delta\to 0^+} -i(2t)^{1/2}, \tag{A10}$$

we find

$$\int_{-iL+\delta}^{z_0+\delta} \mathrm{d}z \, \frac{e^{-i\alpha z}}{(1 - 2iz)^{1/2}} \xrightarrow{\delta\to 0^+} e^{-\alpha/2} \int_{L-1/2}^{0} \mathrm{d}t \, \frac{e^{-\alpha t}}{(2t)^{1/2}}, \tag{A11}$$

which is the same as (A9). After letting $L \to +\infty$, we finally obtain

$$I = \frac{\alpha^2}{3}\sqrt{2}e^{-\alpha/2} \int_0^{+\infty} \mathrm{d}t \, \frac{e^{-\alpha t}}{\sqrt{t}} = \frac{1}{3}\alpha\sqrt{2\pi\alpha}\, e^{-\alpha/2}. \tag{A12}$$

It remains to prove that the integrals over Γ_L and Γ_ϵ are irrelevant. As far as the former is concerned, it suffices to observe that its modulus is bounded from above by

$$\frac{L}{(2L-1)^{1/2}} \int_\pi^{2\pi} \mathrm{d}\theta \, e^{L\alpha \sin\theta} < \frac{2L}{(2L-1)^{1/2}} \int_\pi^{3\pi/2} \mathrm{d}\theta \, e^{2L\alpha(1-\theta/\pi)} = \frac{\pi/\alpha}{(2L-1)^{1/2}}(1 - e^{-L\alpha}), \tag{A13}$$

where we used the inequality

$$\sin\theta < \frac{2}{\pi}(\pi - \theta), \tag{A14}$$

valid for $\pi < \theta < 3\pi/2$. Moreover, we have

$$\left| \int_{\Gamma_\epsilon} \frac{e^{-i\alpha x}}{(1 - 2ix)^{1/2}} \right| \le 2\pi\epsilon \, \frac{e^{-\alpha/2}}{(2\epsilon)^{1/2}}, \tag{A15}$$

which vanishes as ϵ goes to zero.

We checked numerically that the result (A12) is correct by expressing I in the equivalent form

$$I = 2 \int_0^{+\infty} \mathrm{d}x \, \frac{\cos\left(\alpha x - \frac{5}{2} \arctan(2x)\right)}{(1 + 4x^2)^{5/4}} \tag{A16}$$

and computing the integral numerically. Summing up, for $l_{\max} = 2$, we obtain

$$\int_{-\infty}^{+\infty} \mathrm{d}x \, \frac{e^{-i\alpha x}}{(c_2 - 2ix)^{5/2}} = \frac{1}{3}\alpha\sqrt{2\pi\alpha}\, e^{-c_2\alpha/2} \tag{A17}$$

and we get

$$e^{-\beta F_s(V_2,A)} = (36\pi)^{-2/3}\left(\frac{V_2}{a^3}\right)^{-4/3} \times e^{-8\pi\beta\lambda} e^{8\pi\beta\sigma_m\delta_m(3V_2/(4\pi))^{1/3}} e^{-\beta\sigma_m A}\left(\frac{2\pi S_2}{s}\right)^8 \times \frac{1}{3\sqrt{2\pi}}\alpha^{3/2}\, e^{-c_2\alpha/2}, \tag{A18}$$

with $S_2 = 9a^2$, $V_2 = 9a^3/(2\sqrt{\pi})$, and $c_2 = 1 + 48\pi\beta\lambda - 24\sqrt{\pi}\beta\sigma_m\delta_m a$.

It is now easy to check that Eq. (3.11) is fulfilled for $l_{\max} = 2$. From (A18), we get

$$e^{-\beta\Delta\Omega(V_2,A)} = (36\pi)^{-2/3}\left(\frac{V_2}{a^3}\right)^{-4/3} e^{-8\pi\beta\lambda} e^{8\pi\beta\sigma_m\delta_m(3V_2/(4\pi))^{1/3}} e^{V_2\beta\Delta P - \beta\sigma_m S_2} \times \left(\frac{2\pi S_2}{s}\right)^8 \frac{1}{3\sqrt{2\pi}}\alpha^{3/2}\, e^{-(\alpha/2)(1+48\pi\beta\lambda - 24\sqrt{\pi}\beta\sigma_m\delta_m a + 2\beta\sigma_m S_2)}, \tag{A19}$$

and we obtain

$$(36\pi)^{1/3}\left(\frac{V_2}{a^3}\right)^{2/3}\int_0^{+\infty} \mathrm{d}\alpha\, e^{-\beta\Delta\Omega(V_2,A)} = (36\pi)^{-1/3}\left(\frac{V_2}{a^3}\right)^{-2/3} e^{-8\pi\beta\lambda} e^{8\pi\beta\sigma_m\delta_m(3V_2/(4\pi))^{1/3}} e^{V_2\beta\Delta P - \beta\sigma_m S_2} \times \left(\frac{2\pi S_2}{s}\right)^8 \frac{1}{3\sqrt{2\pi}} \times \int_0^{+\infty} \mathrm{d}\alpha\, \alpha^{3/2}\, e^{-(\alpha/2)(1+48\pi\beta\lambda - 24\sqrt{\pi}\beta\sigma_m\delta_m a + 2\beta\sigma_m S_2)}. \tag{A20}$$

Since

$$\int_0^{+\infty} \mathrm{d}x\, x^{3/2}\, e^{-Kx} = \frac{3\sqrt{\pi}}{4} K^{-5/2}, \tag{A21}$$

the final result is

$$\int_0^{+\infty} \frac{\mathrm{d}A}{a^2}\, e^{-\beta\Delta\Omega(V_2,A)} = (36\pi)^{-1/3}\left(\frac{V_2}{a^3}\right)^{-2/3} e^{-8\pi\beta\lambda} e^{8\pi\beta\sigma_m\delta_m(3V_2/(4\pi))^{1/3}} \times e^{V_2\beta\Delta P - \beta\sigma_m S_2}\left(\frac{2\pi S_2}{s}\right)^8 \times \frac{1}{\left(1 + 48\pi\beta\lambda - 24\sqrt{\pi}\beta\sigma_m\delta_m a + 2\beta\sigma_m S_2\right)^{5/2}}, \tag{A22}$$

which indeed is the value of $\exp\{-\beta\Delta\Omega(V_2)\}$ (cf. Eq. (C16) of Ref. 3; note that, due to an oversight, a term $\exp\{\beta\rho_s|\Delta\mu|V\}$ was erroneously included in the expression of Z_s).

There is a more elegant way to obtain Eq. (A18). Upon rewriting Eq. (3.12) as

$$e^{-\beta F_s(V,A)} = (36\pi)^{-2/3}\left(\frac{V}{a^3}\right)^{-4/3} e^{-8\pi\beta\lambda} e^{8\pi\beta\sigma_m\delta_m(3V/(4\pi))^{1/3}} e^{-\beta\sigma_m A}\left(\frac{2\pi S}{s}\right)^3 \times \int_{-\infty}^{+\infty} \prod_{l>1,m}\left(\frac{S}{s}\mathrm{d}x_{l,m}\right) \exp\left(-\frac{1}{4\pi}\sum_{l>1,m} c_l(S)x_{l,m}^2\right)\delta\left(\frac{1}{8\pi}\sum_{l>1,m}(l^2+l-2)x_{l,m}^2 - \alpha\right), \tag{A23}$$

one observes that, by a rescaling of the integration variables, the integral in (A23) is converted to an integral over the surface of a M-dimensional hypersphere, with $M = (l_{\max}+1)^2 - 4$. We readily obtain

$$e^{-\beta F_s(V,A)} = (36\pi)^{-2/3}\left(\frac{V}{a^3}\right)^{-4/3} e^{-8\pi\beta\lambda} e^{8\pi\beta\sigma_m\delta_m(3V/(4\pi))^{1/3}} e^{-\beta\sigma_m A}\left(\frac{2\pi S}{s}\right)^3 \times \prod_{l=2}^{l_{\max}}\left(\frac{8\pi}{l^2+l-2}\right)^{l+1/2}\left(\frac{S}{s}\right)^{2l+1} \times \frac{1}{2\sqrt{\alpha}}\int_{S^M(\sqrt{\alpha})} \mathrm{d}S \exp\left(-\sum_{l>1,m}\frac{2c_l}{l^2+l-2}x_{l,m}^2\right), \tag{A24}$$

where $S^M(\sqrt{\alpha})$ denotes the surface of the M-dimensional hypersphere of radius $\sqrt{\alpha}$. The integral in (A24) is trivial for $l_{\max} = 2$, where we are again led to the result (A18). For $l_{\max} > 2$, the surface integral may still be evaluated numerically by resorting to Monte Carlo sampling,[18] but the computation is feasible only when $l_{\max}$ is not too large.

APPENDIX B: MEAN AREA AND WIDTH OF A QUASISPHERICAL CLUSTER OF FIXED VOLUME

In this appendix, we establish a number of formulae for a quasispherical cluster of fixed volume, which extend to spherical geometry known properties of a rough planar interface.

For a quasispherical interface of volume V, statistical averages are computed with a weight proportional to $\exp\{-\beta\mathcal{H}_s\}\delta(\mathcal{V}[\Sigma]-V)$ with $\mathcal{H}_s$ given by Eq. (2.3). In particular, using Eq. (C2) of Ref. 3, the average interface area reads

$$\langle\mathcal{A}[\Sigma]\rangle_V = S\left(1+\frac{1}{4}\sum_{l=2}^{l_{\max}}\frac{(2l+1)(l-1)(l+2)}{b_l}\right) \quad \text{(B1)}$$

with

$$b_l = 1+\frac{\beta\sigma_m}{2}S(l^2+l-2)-4\pi\beta\sigma_m\delta_m\left(\frac{S}{4\pi}\right)^{1/2}(l^2+l-2) + 2\pi\beta\lambda\, l(l+1)(l-1)(l+2). \quad \text{(B2)}$$

The large-V behavior of (B1) can be extracted by the Euler-Mac Laurin formula, leading eventually to

$$\frac{\langle\mathcal{A}[\Sigma]\rangle_V}{S} = 1+\frac{k_BT}{8\pi\lambda}\ln\left(1+\frac{4\pi\lambda}{\sigma_m a^2}\right) + \frac{2\sqrt{\pi}\delta_m}{\beta\sigma_m a^2+4\pi\beta\lambda}\frac{1}{\sqrt{S}}+\mathcal{O}(S^{-1}) \quad \text{(B3)}$$

(for example, the asymptotic value of $\langle\mathcal{A}[\Sigma]\rangle_V/S$ for $\beta\sigma_m a^2 = 1$ and $\beta\lambda = 0.2$ is 1.249982...). A more elegant way to derive (B3) is to observe that, by Eq. (3.5),

$$\langle\mathcal{A}[\Sigma]\rangle_V = \left.\frac{\partial F_s(V)}{\partial\sigma_m}\right|_{\sigma_m\delta_m}. \quad \text{(B4)}$$

Using Eq. (C21) of Ref. 3, we readily arrive at (B3). We successfully checked Eq. (B3) in a few cases also by directly computing the sum in (B1). In particular, $\langle\mathcal{A}[\Sigma]\rangle_V/S$ indeed approaches its limiting value from above when $\delta_m > 0$.

The result (B3) is akin to

$$\frac{\langle\mathcal{A}\rangle}{L^2}\sim 1+\frac{k_BT}{8\pi\lambda}\ln\left(1+\frac{\lambda\pi^2}{\gamma a^2}\right), \quad \text{(B5)}$$

which applies for a solid-on-solid interface with projected area L^2 and Hamiltonian

$$\mathcal{H}[h] = \gamma L^2+\frac{1}{2}\int_D \mathrm{d}x\,\mathrm{d}y\left[\gamma(\nabla_\perp h)^2+\lambda(\nabla_\perp^2 h)^2\right], \quad \text{(B6)}$$

where $\nabla_\perp = \partial_x\hat{\mathbf{x}}+\partial_y\hat{\mathbf{y}}$ and the integral is extended over a square (the domain D) of area L^2. In Eq. (B5), the characteristic length a arises from the lattice regularization of (B6), which is a necessity if we are to avoid the divergence of the partition function. Observe that the Gaussian interface described by Eq. (B6) is always rough, since

$$\left\langle(h_{\mathbf{x}}-h_{\mathbf{x}'})^2\right\rangle\sim\frac{k_BT}{\pi\gamma}\ln\frac{|\mathbf{x}-\mathbf{x}'|}{a}. \quad \text{(B7)}$$

This latter result is easily translated to the sphere, by observing that the average square width of a quasispherical cluster reads

$$\frac{1}{4\pi}\int\mathrm{d}^2\Omega\,\langle(R(\theta,\phi)-R_0)^2\rangle_V = \frac{S}{2}\sum_{l=1}^{l_{\max}}\frac{2l^2+l+1}{(2l+1)b_l}\sim\frac{k_BT}{3\sigma_m}\ln\left(\frac{V}{a^3}\right). \quad \text{(B8)}$$

Besides certifying that a quasispherical interface is technically rough, Eq. (B8) also indicates that the average size of the deviation $R/R_0-1=\epsilon$ from sphericity scales as $\sqrt{S^{-1}\ln(S/a^2)}$ for large clusters; on the other hand, for the smallest clusters the angular average of $\langle\epsilon^2\rangle_V^{1/2}$ can be as large as 0.6 for typical values of the model parameters. Hence we confirm that the quasispherical model is a near-coexistence approximation only rigorously valid for small to moderate undercooling.

We note in passing that the average cluster area can be put in relation with the *mechanical* surface tension τ,[19] which measures the elastic response of an interface to a change in its projected area. In the planar case (B6), the stretching or shrinking of the projected area is obtained by changing a, the lattice spacing, at fixed number N of lattice sites. The result is

$$\tau\equiv\frac{1}{N}\frac{\partial F_s}{\partial(a^2)} = \gamma\frac{\langle\mathcal{A}\rangle}{L^2}-\frac{k_BT}{2a^2}. \quad \text{(B9)}$$

Similarly, in the quasispherical case τ can be obtained by keeping the total number of (l, m) modes fixed while differentiating $F_s(V)$ with respect to S. Calling $N = (l_{\max}+1)^2 = S/a^2$, we first rewrite F_s as (see Eq. (C18) in Ref. 3)

$$F_s = -2k_BT\ln N+\sigma_m Na^2+8\pi\lambda - 8\pi\sigma_m\delta_m\left(\frac{Na^2}{4\pi}\right)^{1/2}+3k_BT\ln 2 + \frac{k_BT}{2}\sum_{l=2}^{l_{\max}}(2l+1)\left(-2\ln\frac{N}{2}+\ln b_l\right). \quad \text{(B10)}$$

After simple algebra, we get

$$\tau = \sigma_m\left(1-\delta_m\left(\frac{4\pi}{S}\right)^{1/2}\right)\frac{\langle\mathcal{A}[\Sigma]\rangle_V}{S}, \quad \text{(B11)}$$

which nicely recalls Eq. (B9).

APPENDIX C: LARGE-SIZE LIMIT OF THE TWO-DIMENSIONAL SURFACE FREE ENERGY

In Ref. 3, the V-dependent surface free energy of a quasispherical cluster was written as $F_s = \sigma(S)S$, where in the large-size limit $\sigma(S) = \sigma(\infty)+\mathcal{O}(S^{-1/2})$ (see Eq. (C21) of Ref. 3). Similarly, we are here interested in establishing the behavior of $F_s(V, A)$ in the limit where $V\to\infty$ for fixed $\alpha = A/S-1$. A likely possibility, suggested by the profiles of $F_s(V,\alpha)$ for increasing V values (see Fig. 6), is that

$$\beta F_s(V,\alpha) = f(\alpha)S+g(\alpha)o(S), \quad \text{(C1)}$$

denoting $o(S)$ a quantity growing slower than S for $S\to\infty$ and f, g two not further specified functions of α. Figure 6 indicates that $f(\alpha)$ has a minimum value, $f_{\min} = f(\alpha_{\min})$, falling not far away from the asymptotic value of $\langle\mathcal{A}[\Sigma]\rangle_V/S-1$. By the same F_s data reported in Fig. 6 we infer that the first subdominant term in (C1) is actually a $\sqrt{S}$ term.

Assuming that (C1) holds, we now prove that $f_{\min} = \beta\sigma(\infty)$. Starting from Eq. (3.11), which we reshuffle as

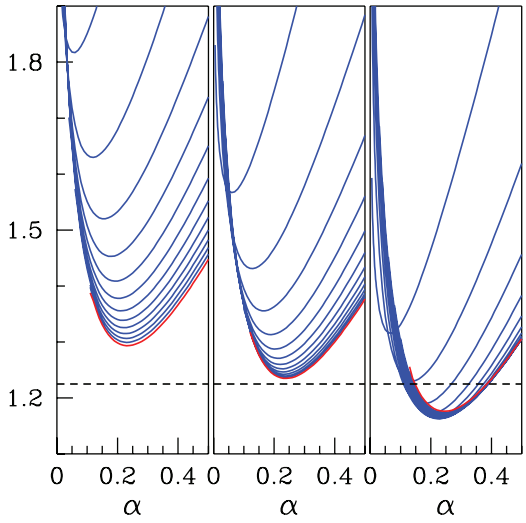

FIG. 6. Ratio of $\beta F_s(V,\alpha)$ to S for increasing V values ($V/a^3 = (l_{\max}+1)^3/\sqrt{36\pi}$ with $l_{\max} = 2, \ldots, 14$). Low V values are on top, and the red curve refers to $l_{\max} = 14$. Three sets of parameters were investigated: $\beta\sigma_m a^2 = 1$, $\beta\lambda = 0.2$, and $\delta_m = -0.1$, 0, 0.1 (from left to right). Upon increasing V, $\beta F_s(V,\alpha)/S$ approaches a limiting profile whose minimum coincides with $\beta\sigma(\infty)$ (the dashed line). For $\delta_m > 0$, the approach to this limit is non-monotonic.

$$-\ln\int_S^{+\infty}\frac{dA}{a^2}\,e^{-\beta F_s(V,A)} = \beta F_s(V), \tag{C2}$$

we divide each side of (C2) by S and then bring the volume to infinity:

$$-\lim_{V\to\infty}\frac{1}{S}\ln\int_0^{+\infty}d\alpha\,\frac{S}{a^2}e^{-\beta F_s(V,\alpha)} = \beta\sigma(\infty). \tag{C3}$$

Upon carrying the limit inside the integral (which is allowed in so far as α is independent of V), the left-hand side of (C3) becomes

$$-\lim_{V\to\infty}\frac{1}{S}\ln\int_0^{+\infty}d\alpha\,e^{-f(\alpha)S-g(\alpha)o(S)}, \tag{C4}$$

in turn equal to $f_{\min}$ by the Laplace (saddle-point) method. Alternatively, we may also expand for large S both f and g to second-order in the deviation of α from $\alpha_{\min}$. By matching the two sides of Eq. (C2), we again find $f_{\min} = \beta\sigma(\infty)$ and moreover (by Eq. (C21) of Ref. 3)

$$g(\alpha_{\min}) = -2\delta_m\sqrt{\pi}\left[2\beta\sigma_m + \frac{\sigma_m}{4\pi\lambda}\ln\left(1+\frac{4\pi\lambda}{\sigma_m a^2}\right)\right]. \tag{C5}$$

The above result can be taken as the proof that the slope of $-\beta\Delta\Omega^*$ at vanishing undercooling is the same for both one and two-CV descriptions of nucleation. In fact, let it be assumed that ΔP is so low that we are authorized to take $\beta F_s(V,\alpha) = f(\alpha)S$. Then, the extremal point (saddle point) of $\Delta\Omega(V,\alpha) = -V\Delta P + F_s(V,\alpha)$ is the unique solution to

$$f'(\alpha) = 0 \quad \text{and} \quad -\beta\Delta P + \frac{2}{3}(36\pi)^{1/3}f(\alpha)V^{-2/3} = 0, \tag{C6}$$

giving eventually

$$R^* \equiv \left(\frac{3V^*}{4\pi}\right)^{1/3} = \frac{2\sigma(\infty)}{\Delta P} \quad \text{and} \quad \Delta\Omega^* = \frac{16\pi}{3}\frac{\sigma(\infty)^3}{(\Delta P)^2}. \tag{C7}$$

These values of critical radius and barrier height are the same occurring in CNT when the interface tension is chosen to be $\sigma(\infty)$.

[1] See, for example, D. Kashchiev, *Nucleation: Basic Theory with Applications* (Butterworth-Heinemann, Oxford, 2000).
[2] S. Prestipino, A. Laio, and E. Tosatti, Phys. Rev. Lett. **108**, 225701 (2012).
[3] S. Prestipino, A. Laio, and E. Tosatti, J. Chem. Phys. **138**, 064508 (2013).
[4] M. P. A. Fisher and M. Wortis, Phys. Rev. B **29**, 6252 (1984).
[5] A. C. Pan and D. Chandler, J. Phys. Chem. B **108**, 19681 (2004).
[6] D. Moroni, P. R. ten Wolde, and P. G. Bolhuis, Phys. Rev. Lett. **94**, 235703 (2005).
[7] F. Trudu, D. Donadio, and M. Parrinello, Phys. Rev. Lett. **97**, 105701 (2006).
[8] B. Peters and B. L. Trout, J. Chem. Phys. **125**, 054108 (2006).
[9] T. Zykova-Timan, C. Valeriani, E. Sanz, D. Frenkel, and E. Tosatti, Phys. Rev. Lett. **100**, 036103 (2008).
[10] W. Lechner, C. Dellago, and P. G. Bolhuis, Phys. Rev. Lett. **106**, 085701 (2011).
[11] J. Russo and H. Tanaka, Sci. Rep. **2**, 505 (2012).
[12] P. R. ten Wolde and D. Frenkel, J. Chem. Phys. **109**, 9901 (1998).
[13] R. K. Bowles, R. McGraw, P. Schaaf, B. Senger, J.-C. Voegel, and H. Reiss, J. Chem. Phys. **113**, 4524 (2000).
[14] L. Maibaum, Phys. Rev. Lett. **101**, 019601 (2008).
[15] P. R. ten Wolde, M. J. Ruiz-Montero, and D. Frenkel, Faraday Discuss. **104**, 93 (1996).
[16] T. Burkhardt, J. Phys. A **14**, L63 (1981).
[17] M. Franke, A. Lederer, and H. J. Schöpe, Soft Matter **7**, 11267 (2011).
[18] W. Krauth, *Statistical Mechanics: Algorithms and Computations* (Oxford University Press, Oxford, 2006).
[19] A. Imparato, J. Chem. Phys. **124**, 154714 (2006).